Pendant Homopolymer and Copolymers as Solution-Processable Thermally Activated Delayed Fluorescence Materials for Organic Light-Emitting Diodes

Zhongjie Ren,[†] Roberto S. Nobuyasu,[‡] Fernando B. Dias,[‡] Andrew P. Monkman,[‡] Shouke Yan[†] and Martin R. Bryce[#]**

[†] *State Key Laboratory of Chemical Resource Engineering, Beijing University of Chemical Technology, Beijing 100029, China. E-mail: skyan@mail.buct.edu.cn*

[‡] *Department of Physics, Durham University, South Road, Durham, DH1 3LE, UK.*

[‡] *Department of Chemistry, Durham University, South Road, Durham, DH1 3LE, UK. E-mail: m.r.bryce@durham.ac.uk*

ABSTRACT. Materials that display thermally activated delayed fluorescence (TADF) have recently been identified as the third generation emitters for organic light-emitting diodes (OLEDs). However, there are only a few reported examples of polymeric TADF materials. This study reports a series of polymers with an insulating backbone and varying ratios of 2-(10*H*-phenothiazin-10-yl)dibenzothiophene-*S*,*S*-dioxide as a pendant TADF unit. Steady-state and time-resolved fluorescence spectroscopic data confirm the efficient TADF properties of the polymers. Styrene, as a co-monomer, is shown to be a good dispersing unit for the TADF groups, by greatly supressing the internal conversion and triplet-triplet annihilation. Increasing the styrene content within the copolymers results in relatively high triplet energy, small energy splitting between the singlet and triplet states (ΔE_{ST}) and a strong contribution from delayed fluorescence to the overall emission. Green emitting OLED devices employing these polymers as spin-coated emitting layers give high performance, which is dramatically enhanced in the copolymers compared to the homopolymer. Within the series, **Copo1** with a regiorandom ratio of 37% TADF units : 63% styrene units displays the best performance with a maximum external quantum efficiency (EQE) of 20.1% and EQE at 100 cd m^{-2} of 5.3%.

INTRODUCTION

Organic light-emitting diode (OLED) devices have been in continous development since the early 1960s.[1-3] To improve the external quantum efficiency (EQE) of OLEDs, extensive studies have focused on synthesizing new emissive materials.[4-7] One of the most important challenges in this field stems from the fact that fluorescent materials harvest emission only from singlet excitons and thus have the limitation of reaching a maximum internal quantum efficiency (IQE) of 25%, whereas statistically 75% triplet excitons are wasted.[8] Harvesting triplet excitons is therefore crucial to achieve OLED devices with 100% IQE. In contrast to pure fluorescent emitters, phosphorescent materials produce light by utilizing both triplet and singlet excitons resulting in almost 100% IQE.[9-11] However, phosphorescent materials incorporate expensive and scarce metals such as iridium or platinum and display significant degradation in the blue spectral region.[12,13] Metal-free, thermally activated delayed fluorescence (TADF) materials are considered to be third-generation emitters for OLEDs.[14-18] The basic requirement for efficient TADF is that the highest occupied and lowest unnocupied molecular orbital (HOMO and LUMO, respectively) are spacially separated to achieve a small energy gap between the lowest lying singlet and triplet states. In this way, both triplet and singlet excitons are utilized via thermal up-conversion of the lowest excited triplets (T_1) to singlets (S_1) together with fluorescence from the S_1 state, leading to a potential IQE of up to 100%.

Small molecules have been extensively investigated in this context and some very high efficiency TADF OLEDs have been reported. For example, 10,10'-(sulfonylbis(4,1-phenylene))bis(9,9-dimethyl-9,10-dihydroacridine) (DMAC-DPS) emits in the blue region with 19.5% EQE.[19] A maximum EQE of 28.6% was obtained in the green region by Lee's group.[20] However, complicated vacuum deposition techniques and precise processing controls are required for many small-molecule based devices to ensure high reproducibility. Solution-

processing techniques, such as spin-coating or inkjet-printing, offer the advantages of lower cost, simpler processability and large area device fabrication.[21,22] Solution processing has been applied successfully to a few small-molecule TADF OLEDs based on 2,4,5,6-tetra(3,6-di-*tert*-butylcarbazol-9-yl)-1,3-dicyanobenzene (t4CzIPN) and close analogs.[23,24]

Polymeric TADF emitters are particularly suitable for solution processing technologies. However, synthesizing TADF oligomers and polymers is challenging and there are no clear guidelines for their optimal molecular structures. Firstly, simultaneously achieving a small energy splitting between the singlet and triplet states (ΔE_{ST}) and suppressing internal conversion is very difficult in molecules containing numerous atoms. Secondly, the triplet population in polymers is easily quenched by intramolecular and intermolecular triplet-triplet annihilation.[25] Nonetheless, significant progress has been made recently and the following examples place the present work in context. Albrecht *et al.*[26] reported TADF in films of solution-processable, non-doped carbazole-based dendrimers with a triazine core: OLED devices with a G3 dendrimer (21 carbazole units) as the active emitting layer gave green electroluminescence with EQE_{max} of 3.4% and a maximum luminance of >1000 cd m^{-2}. Nikolaenko *et al.*[27] reported a linear TADF polymer obtained by a block polymerization approach of three monomers with triazene-amine-triazene emitter units of various lengths spaced with non-conjugated segments. No information was given on the molecular weight or polydispersity of the material. The polymer showed EQE_{max} of 10% at very low current densities and green emission with EQE >4.5% at 100 cd m^{-2}. Yang *et al.*[28] synthesized copolymers from three monomer components, with a backbone of polycarbazole and 10-(4-(5-phenyl-1,3,4-oxadiazol-2-yl)phenyl)-10*H*-phenoxazine as pendant TADF units. The most efficient copolymer in the series had a low molecular weight of 3280 with polydispersity index (PDI) 1.77; EQE_{max} of 4.3%; EQE 2.4% at 100 cd m^{-2} and maximum power efficiency 11.2 lm W^{-1} was obtained for bluish-green emission. Very recently Lee *et al.*[29] reported two polymers with a backbone consisting of alternating electron donating units (carbazole in

pCzBP, or acridine in pAcBP) and accepting benzophenone (BP) units. The molecular weights were in the range 8.7-9.2 × 10^4 (PDI 1.2-1.5). A green pCzBP OLED had EQE_{max} of 8.1 ± 0.7%, maximum current efficiency of 24.9 ± 1.7 cd A^{-1} and maximum power efficiency of 9.0 ± 0.7 lm W^{-1} at low luminance. A yellow pAcBP device had higher performance with EQE_{max} of 9.3 ± 0.9% and 8% at 1000 cd m^{-2}, maximum current efficiency of 31.8 ± 1.1 cd A^{-1} and maximum power efficiency of 20.3 ± 1.8 lm W^{-1}. Zhu *et al*. reported a TADF polymer with donor (carbazole) and acceptor (9,10-dihydroacridine) as backbone and pendant units, respectively. The polymer PAPTC had M_n 22.0 kDa and PDI 2.96. A green OLED with EQE_{max} of 12.6% at 180 cd m^{-2} was obtained.[30]

We identified the donor-acceptor (D-A) structure 2-(10*H*-phenothiazin-10-yl)dibenzothiophene-*S*,*S*-dioxide (PTZ-DBTO2) as an efficient TADF unit and recently reported preliminary data on the incorporation of this unit into polymeric structures.[31] OLEDs fabricated with a conjugated copolymer based on PTZ-DBTO2 and dibenzothiophene blocks as the active layer achieved EQE_{max} 11.05% and 3.5% at 100 cd m^{-2}. **Copo1** (Scheme 1) with pendant PTZ-DBTO2 units gave considerably lower device efficiencies with EQE_{max} 2.5%. [31]

In the present work, we report in detail the properties and OLED performance of three copolymers, **Copo1**, **Copo2** and **Copo3**. The copolymers comprise different ratios of PTZ-DBTO2 and styrene units and were designed to study the effect of PTZ-DBTO2 content on the TADF properties. Styrene was chosen as a cheap and readily available monomer to provide spacer units between the pendant TADF groups in the copolymers, thereby reducing the intramolecular and intermolecular triplet-triplet annihilation of adjacent TADF units. The PTZ-DBTO2 homopolymer (**Homopo**) is also studied for comparison. Steady-state and time-resolved fluorescence spectroscopic data confirm the TADF properties of the polymers. The OLED device data demonstrate that the copolymers give dramatically better performance than the homopolymer, establishing the benefit of minimizing interactions of the TADF units.

Green-emitting devices of **Copo1** achieve EQE_{max} as high as 20.1%, with EQE 5.3% at 100 cd m^{-2}.

RESULTS AND DISCUSSION

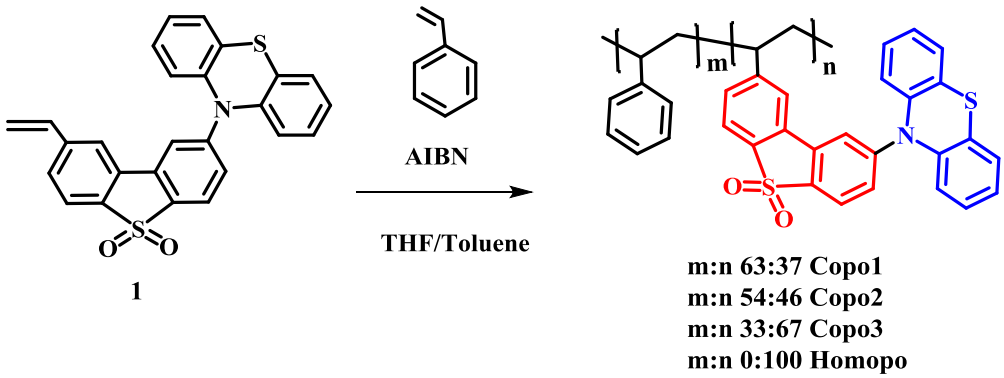

Scheme 1. Synthetic route for **Copo1-3** and **Homopo** with pendant PTZ-DBTO2 TADF units comprising donor phenothiazine (blue) and acceptor dibenzothiophene-*S*,*S*-dioxide (red).

As depicted in **Scheme 1**, the **Copo1-3** and the homopolymer were prepared by the radical polymerization of styrene and 2-(10*H*-phenothiazin-10-yl)-8-vinyldibenzothiophene-*S*,*S*-dioxide **1**[31] with molar feed ratios of 80:20, 70:30, 50:50 and 0:100, respectively. The ratios of the styrene and TADF units in the copolymers were estimated from elemental analysis data to be 63:37, 54:46, and 33:67 for **Copo1-3**, respectively, indicating the higher reactivity of TADF monomer **1** compared to styrene in the copolymerization reaction. The four polymers are all readily soluble in common organic solvents, such as dichloromethane, THF, and chlorobenzene. They are therefore suitable for thin film formation using spin-coating, dipping, and casting techniques. The structures of the polymers were characterized by ^{1}H NMR spectroscopy (Figures S1-S4) and elemental analysis. The weight average molecular weights (M_w) and PDI of the polymers were determined to be 11.5 kDa, PDI 1.6 for **Copo1**, 12.7 kDa, PDI 1.7 for **Copo2**, 15.6 kDa, PDI 1.9 for **Copo3**, and 41.0 kDa, PDI 2.5 for **Homopo**, by gel permeation chromatography (GPC) in THF with polystyrene as standard

(Table 1). These data confirm that polymers with moderately high molecular weights are obtained.

The thermal properties of the polymers were investigated by differential scanning calorimetry (DSC) and thermogravimetric analysis (TGA). As shown Table 1, the decomposition temperatures (T_d) under nitrogen are in the range 400 - 419 ^oC, showing their excellent thermal stability. A trend is that T_d decreases slightly with an increased ratio of styrene units. Figure 1a and Table 1 shows that a distinct glass transition temperature (T_g) is observed for each polymer with values ranging from at 217 ^oC for **Copo1** to 269 ^oC for **Homopo**. The high T_g should endow the polymers with long-term stability. In addition, there are no observed exothermic peaks resulting from crystallization during the scan ranges for all the polymers, indicating an excellent amorphous glass state stability.[32]

Table 1. Characterization data for the polymers.

	M_w/ PDI	HOMO (eV)	LUMO (eV)	E_g (eV)	T_g (^oC)	T_d (^oC)	ΔE_{ST} (eV)	E_T (eV)	DF ratio
Copo1	11,500/1.6	-5.31	-3.10	2.21	217	400	0.35	2.46	44.4%
Copo2	12,700/1.7	-5.33	-3.06	2.27	229	412	0.46	2.30	35.6%
Copo3	15,600/1.9	-5.42	-3.06	2.36	252	414	0.42	2.30	34.5%
Homopo	41,000/2.5	-5.43	-3.05	2.39	269	419	0.40	2.27	33.2%

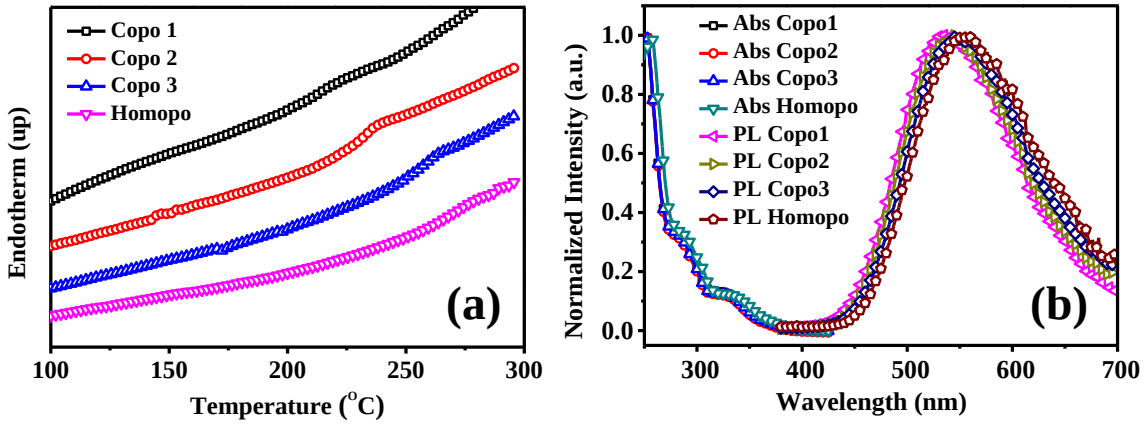

Figure 1. (a) DSC curves. (b) UV-absorption and PL spectra of **Copo1-3** and **Homopo** in pristine thin films.

The UV-Vis absorption spectrum of **Homopo** (Figure 1b) shows the main characteristic peaks located at ca. 285 and 330 nm, which are consistent with the absorption spectrum of the PTZ-DBTO2 TADF units.[31] The absorption profiles for **Copo1-3** are similar and are blue-shifted by ca. 6-7 nm compared to **Homopo**. This indicates that the styrene units can effectively reduce any aggregation between the TADF units and should thereby reduce the triplet-triplet annihilation. The fluorescence spectra appear as broad and featureless bands with λ_{max} at 535, 546, 553 and 556 nm for **Copo1**, **Copo2**, **Copo3** and **Homopo**, respectively. An obvious and incremental red-shift can be observed when the content of styrene decreases. This is probably due to an interaction between the TADF units. In **Copo1**, with the larger proportion of styrene spacers, the TADF units behave more as an isolated chromophore, and therefore the phosphorescence is at higher energy, because of a more substantial acceptor contribution. This is consistent with our previous report.[31] In addition, the peak widths at half height of all the emissions are decreased from ca.141 nm for **Homopo** to 128 nm for **Copo1**, suggesting the addition of styrene can reduce aggregation and improve the color purity. The PL data are consistent with the UV-Vis absorption spectra.

The electrochemical behavior of the four polymers was investigated by cyclic voltammetry (CV) in degassed anhydrous acetonitrile solution. The data show quasi-reversible oxidation and reduction processes for all polymers (**Figure 2**) corresponding to electrochemical doping and dedoping during the potential sweeps. **Copo1** has very similar oxidation and reduction potentials to unsubstituted phenothiazine donor and dibenzothiophene-*S*,*S*-dioxide acceptor units, respectively.[30] All the polymers display similar oxidation and reduction behavior as the process is centered on the PTZ-DBTO2 TADF units. A slight increase in oxidation potential is observed when the content of styrene decreases, i.e. **Homopo** is harder to oxidize than the copolymers, which may be attributed to the relatively higher conjugation of **Homopo** which is consistent with the absorption spectra discussed above. Meanwhile, **Homopo** is more difficult to reduce than the copolymers. This is possibly

due to the enhanced steric congestion in **Homopo** which could make it more difficult to flatten the structure of the polymer chains during the electron transfer process.

The HOMO and LUMO energy levels of all the polymers were calculated according to the internal reference ferrocene redox couple in acetonitrile by using the following formulae: [33,34]

$$E_{HOMO} = -(E_{(onset,\ ox\ vs.\ Fc+/Fc)} + 5.1) \quad (1)$$

$$E_{LUMO} = -(E_{(onset,\ red\ vs.\ Fc+/Fc)} + 5.1) \quad (2)$$

The HOMO and LUMO energy levels are shown in Table 1. There are two clear trends in these data: as the content of styrene units is reduced (i) the HOMO level decreases and the LUMO level increases; (ii) the electrochemical band gap increases incrementally, from 2.21 eV for **Copo1** to 2.39 eV for **Homopo**.

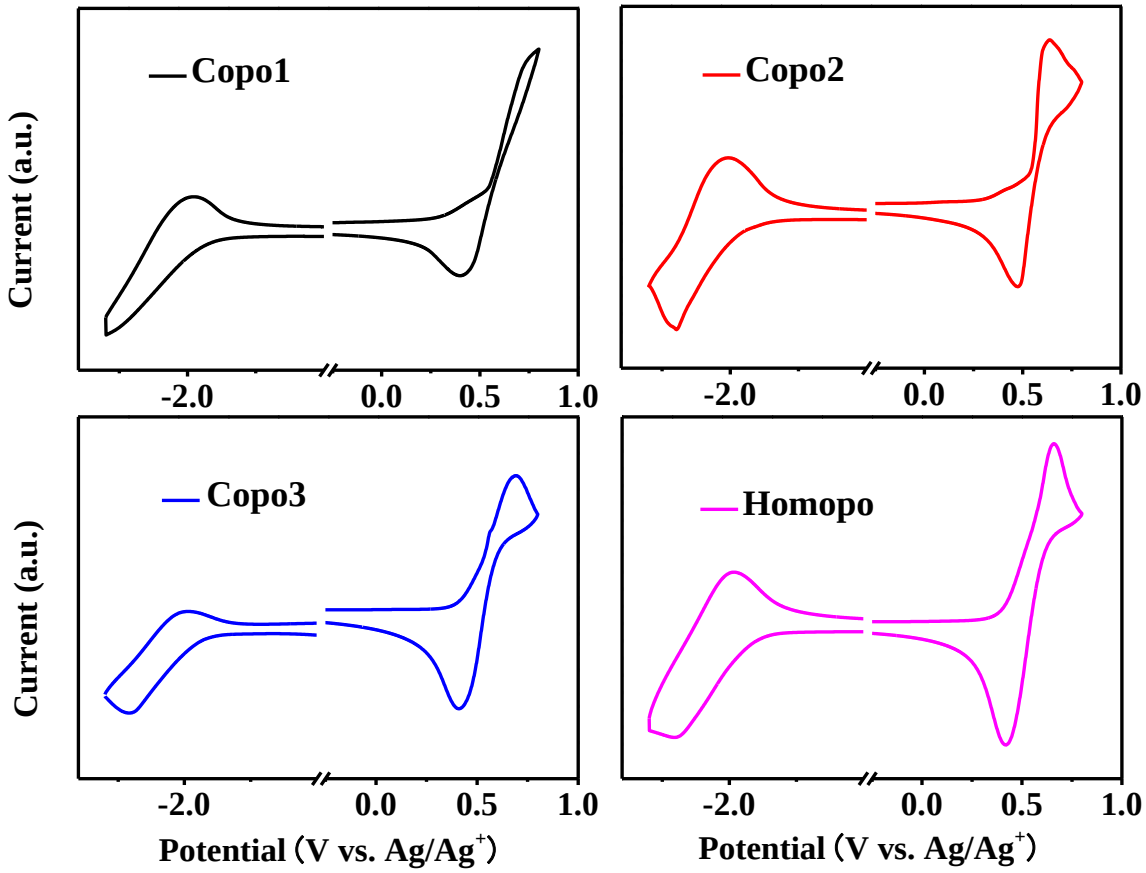

Figure 2. Cyclic voltammograms of **Copo1-3** and **Homopo** in acetonitrile.

To detect the triplet emission, quenching experiments of the emission with oxygen were performed. The emissions of all the polymers dispersed in zeonex matrix show higher intensity in vacuum than in oxygen. The overall luminescence of the PTZ-DBTO2 units in the polymers has a strong contribution from the triplet state (TADF). Oxygen is a well-known triplet quencher, which explains why the emission increases in vacuum. Moreover, the calculated emission ratio ($\frac{I_{Vac}}{I_{O2}} = \frac{I_{PF} + I_{DF}}{I_{PF}} = \frac{I_{DF}}{I_{PF}} + 1$) decreases with a reduction in the content of styrene units, where PF and DF are prompt and delayed fluorescence, respectively. For example, the I_{DF}/I_{PF} ratio decreases from 0.35 in **Copo1** to 0.17 in **Homopo** as shown in Figure S5, which may be assigned to the styrene units dispersing the TADF units and thus preventing triplet-triplet annihilation.

The fluorescence decays in film state of **Copo1-3** and **Homopo** at room temperature were monitored over a time interval of six decades (**Figure 3a**). Both PF and DF components are clearly observed for all the polymers. However, PF and DF show complex decay dynamics. The decays cannot be fitted by sums of exponentials. This is probably due to dispersion on the TADF barrier. **Figure 3b** shows the typical excitation power dependence of DF of **Copo2** at room temperature. The emission intensity increases linearly with excitation dose as predicted in a TADF mechanism. Figure 3c shows the integrated delayed fluorescence collected with 1 μs delay time, and integrated over 100 μs; a clear linear dependence with excitation dose (the slope is 1) is observed. These data confirm that DF originates from a monomolecular process, rather than from triplet-triplet annihilation (for which the slope is 2).[35] Therefore, the DF of **Copo2** is unambiguously assigned to a TADF mechanism. **Copo1**, **Copo3** and **Homopo** show similar behavior (Figure S6-8). **Figure 3d** presents the typical dependence with temperature of the fluorescence decay of **Copo2**. It is clear that the PF component shows no variation with temperature. However, the threshold delay time at which TADF significantly deviates from the PF decay increases with reducing temperature.

Moreover, the lifetime of delayed fluorescence in **Copo2** increases with decreasing temperature. These observations are consistent with a longer triplet lifetime at lower temperatures due to a slower reverse intersystem crossing rate. All these observations are consistent with the TADF mechanism, and are also observed in **Copo1**, **Copo3** and **Homopo** as shown in **Figures S9-S11.**

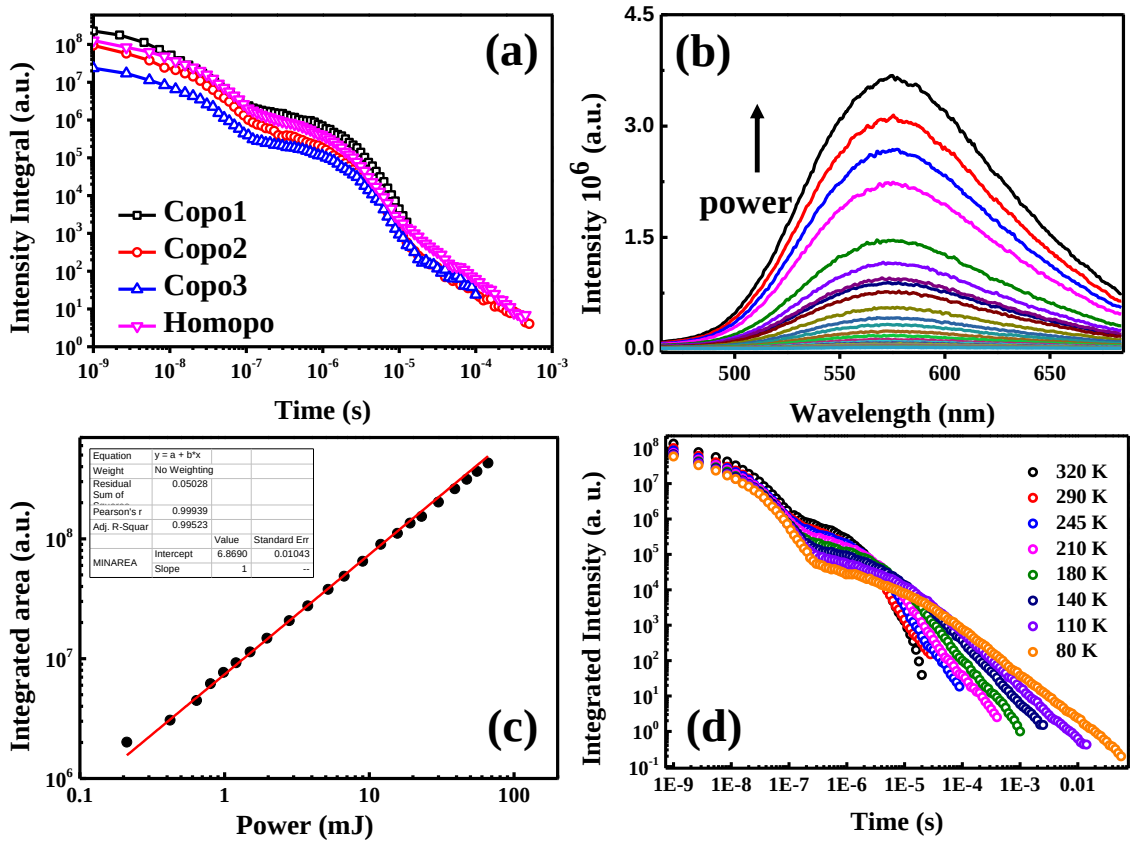

Figure 3. (a) Fluorescence decay data for **Copo1-3** and **Homopo**, collected in pristine thin films at room temperature. (b) Power dependence of the PL spectra for **Copo2**. (c) TADF of **Copo2** showing linear dependence with excitation power. (d) Temperature dependence of **Copo2** fluorescence decays.

We have previously reported in preliminary studies that **Copo1** gave OLEDs with EQE_{max} 2.5%.[31] To explore the structure-property relationships of **Copo1-3** and **Homopo** in polymer OLEDs, and to optimize the device performance within this series, devices were fabricated with the following architecture: indium tin oxide (ITO)/PEDOT:PSS (40 nm)/ 10% **Copo1-3** or **Homopo** and 90% 1,3-bis(carbazol-9-yl)benzene (mCP) (45 nm)/ 1,3,5-tris(1-

phenyl-1*H*-benzimidazol-2-yl)benzene (TPBi) (30 nm)/ LiF (1 nm)/Al (100 nm), where poly(3,4-ethylenedioxythiophene):poly(styrenesulfonic acid) (PEDOT:PSS) serves as the hole-injection layer; TPBi acts as the electron-transporting layer and 10% **Copo1-3**, **Homopo** and 90% mCP in chlorobenzene was spin-coated to form the emitting layer. Current density-voltage and brightness-voltage curves are shown in **Figures 4a,b**. Except for **Homopo**, all the copolymers reach a maximum luminance of 1000 cd/m^2. All of the devices exhibit driving voltages in the range of 5.8-7.4 V (recorded at a luminance of 10 cd m^{-2}). Notably, **Copo1** displays a lower turn-on voltage of 5.8 V compared with the other polymers, and the driving voltages increase with increasing the content of TADF units. This may be attributed to the relatively low LUMO of **Copo1**, which is beneficial to electron injection. **Figures 4c,d** depict power, current efficiencies and the external quantum efficiency plotted with respect to current density. The key EL parameters are summarized in **Table 1**. The best EL performance is achieved for the **Copo1**-based device with CE_{max} of 61.3 cd/A, PE_{max} of 40.1 lm/W, and EQE_{max} of 20.1%. Furthermore, at the practically-relevant brightness of 100 cd m^{-2} the EQE was 5.3%. Compared with previous data for **Copo1**[31] it is clear that mCP is a better host than CBP. This is most likely due to the fact that the triplet level of mCP (2.9 eV)[36] is higher than that of CBP (2.56 eV),[36] which helps to confine the triplet excited states in the TADF units when mCP is the host. This will avoid quenching due to triplet-triplet annihilation, and also quenching by the host. The device performances for **Copo2**, **Copo3** and **Homopo** in directly comparable conditions are relatively low, indicating the insulating spacer styrene units play an important role in the OLED properties of these polymers.

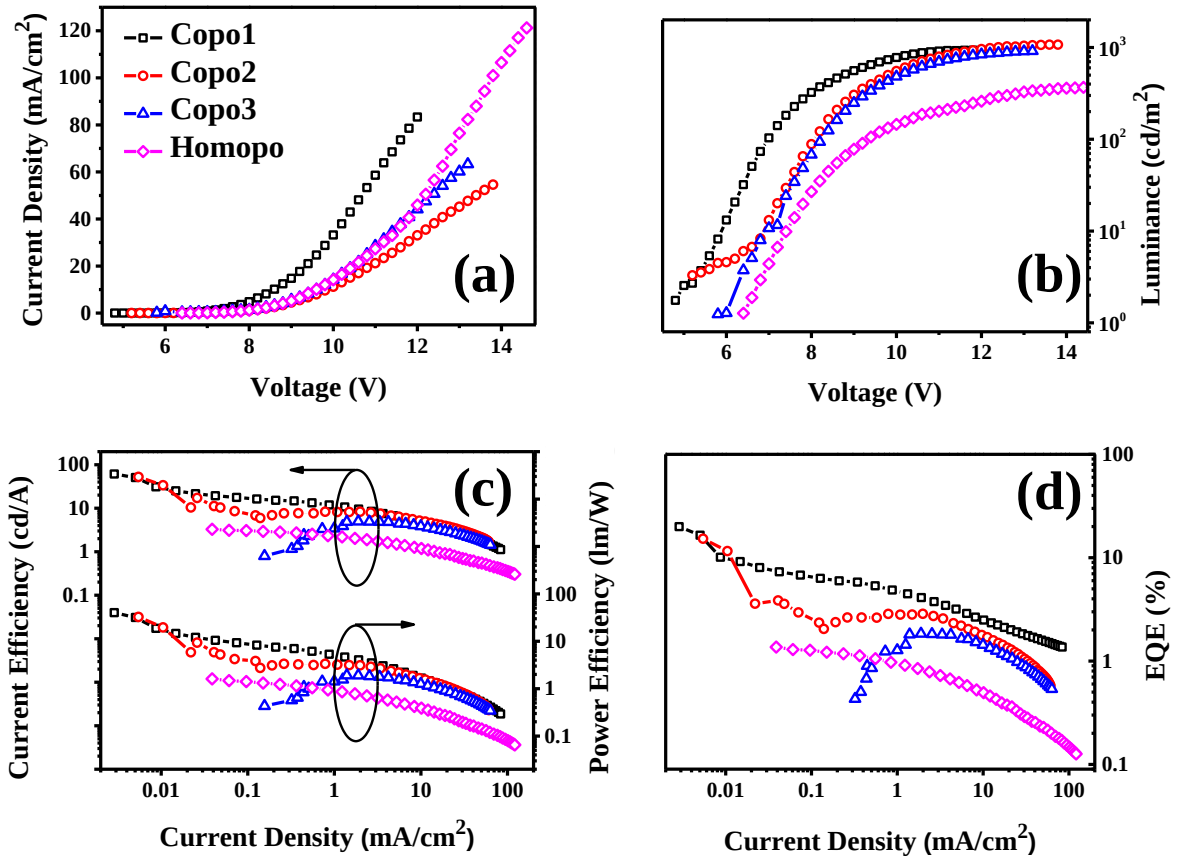

Figure 4. Characteristics of OLED devices for **Copo1-3** and **Homopo** (a) current density versus voltage. (b) luminance versus voltage. c) current and power efficiency versus current density. d) EQE versus current density.

The electroluminescence spectra of the polymers are shown in **Figure 5a**. All of the devices exhibit emission exclusively from the TADF polymers at ca. 530-550 nm without any evidence of mCP emission at 360 nm.[37] It is notable that the λ_{max} value of the EL spectra shifts to longer wavelength in the sequence **Copo1** (533 nm) < **Copo2** (536 nm) < **Copo3** (539 nm) < **Homopo** (556 nm). The EL spectrum of **Copo1** is very close to the TADF monomer units (PL peak at 529 nm), indicating styrene units are vital to prevent aggregation and improve color purity. Therefore, a consistent change of CIE coordinates for the devices can be seen from (0.36, 0.55) for **Copo1** to (0.43, 0.51) for **Homopo** (Table 2).

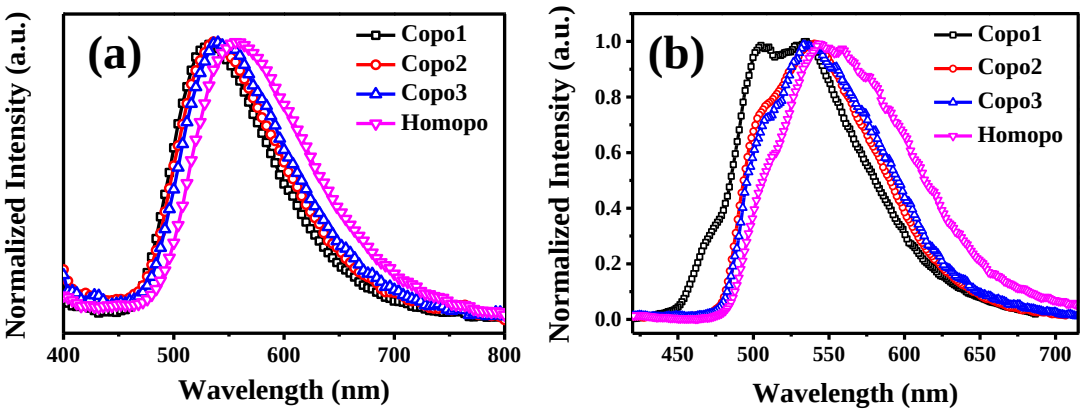

Figure 5. (a) Electroluminescent spectra; (b) Phosphorescent spectra of **Copo1-3** and **Homopo**.

Table 2. Device performance data.

	V_{10} [a] (V)	λ_{max} [b] (nm)	EQE_{100} [c] (%)	EQE_{max} [d] (%)	CE_{max} [e] (cd/A)	PE_{max} [f] (lm/W)	CIE [g] (x, y)
Copo1	5.8	533	5.3	20.1	61.3	40.1	(0.36, 0.55)
Copo2	6.8	536	2.8	15.2	52.5	32.6	(0.37, 0.53)
Copo3	6.9	539	1.8	1.8	5.0	1.9	(0.39, 0.53)
Homopo	7.4	556	0.6	1.4	3.3	1.6	(0.43, 0.51)

[a] The driving voltage at 10 cd m^{-2}. [b]EL peak wavelength. [c]External quantum efficiency at 100 cd m^{-2}. [d]Maximum external quantum efficiency. [e]Maximum current efficiency. [f]Maximum power efficiency. [g]The Commission Internationale de L'Eclairage coordinates.

To elucidate the reason why **Copo1** based OLEDs display the best performance in this series, the triplet energies of the four polymers were determined as shown in **Figure 5b** according to the phosphorescent spectra for which the highest energy peak defines the triplet energy (E_T).[14] As shown in **Table 1**, **Copo1** has the highest E_T (2.46 eV) and E_T decreases with decreasing the content of styrene. Styrene units have low polarity, therefore the different polymer compositions should have a minimal effect on the dielectric properties of the system. Moreover, the triplet state is a local excited state, with negligible excited dipole moment and therefore is not significantly affected by the dielectric medium. Since the energy of the singlet state is not so affected, the singlet-triplet energy gap is smaller in **Copo1** than in the other polymers, which facilitates reverse intersystem crossing (RISC) and leads to a higher TADF contribution in **Copo1**. The singlet energy is estimated from the onset of the broad

emission band, which provides a more comparable result, as demonstrated by previous studies.[38,39] The ΔE_{ST} values for **Copo1-3** and **Homopo** are calculated to be 0.35, 0.46, 0.42 and 0.40 eV, respectively. It is well known[14-18] that a small ΔE_{ST} is necessary for efficient RISC which is required for TADF, and the smaller the value of ΔE_{ST}, the higher the rate of RISC. This systematic change in ΔE_{ST} in the current series of polymers correlates with their OLED performance.

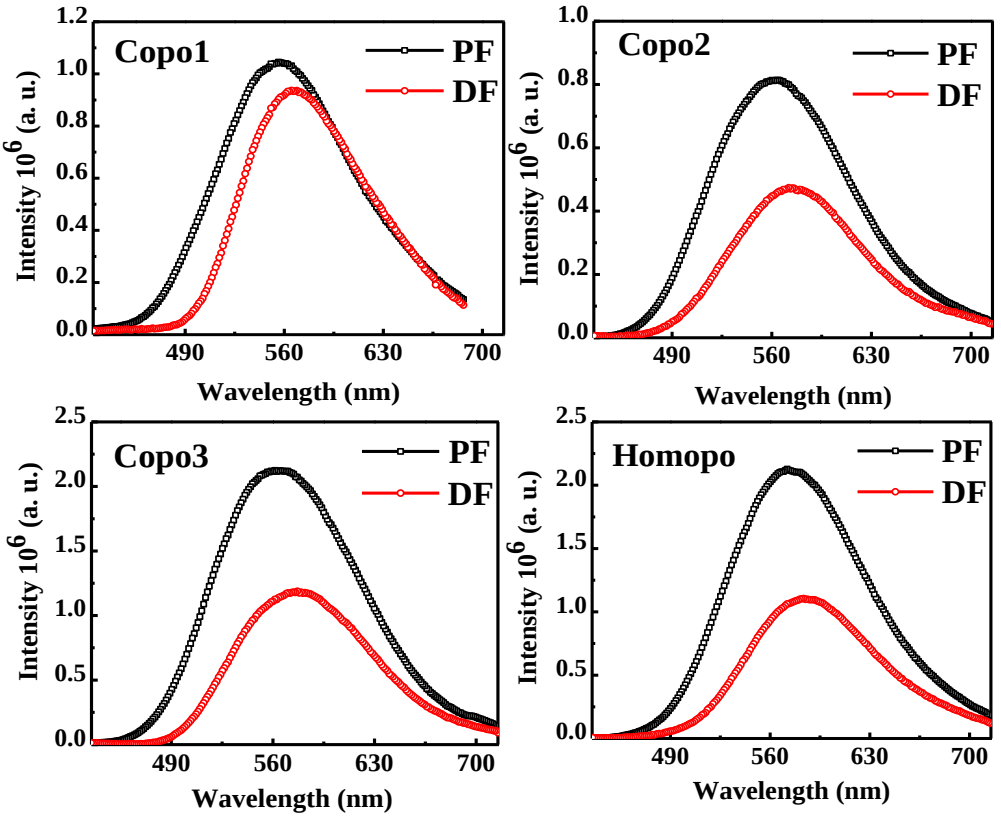

Figure 6. Integration of the prompt and delayed fluorescence (PF and DF) of **Copo1-3** and **Homopo** based on the fluorescence decays in vacuum.

The contribution of delayed fluorescence (DF) to the overall emission is shown in **Figure 6** for all the polymers. The data were obtained from the integral of the prompt and delayed fluorescence, determined from the luminescence decay obtained in vacuum because the pristine films are not permeable to oxygen diffusion. For all the polymers, the DF of is red shifted compared with the PF, and the DF shows an obvious spectral narrowing relative to PF

(**Figure 6ba-d**). This may be caused by the contributions of a residual local singlet excited state and a singlet charge transfer state in PF. As stated in **Table 1**, the DF contribution is 44.4% for **Copo1** and this value decreases gradually with reducing the content of styrene to 33.2% for **Homopo**. These data are in good agreement with the determination from steady-state fluorescence, and with the enhanced performance of **Copo1** devices.

CONCLUSIONS

In summary, a series of pendant polymers with 2-(10*H*-phenothiazin-10-yl) dibenzothiophene-*S*,*S*-dioxide as TADF units and insulating styrene units as side chains have been synthesized and structure/property/OLED performance relationships have been established. Photophysical data confirm that for all the polymers the reverse intersystem crossing mechanism is able to compete with internal conversion and triplet-triplet annihilation. The effect of styrene content on the properties of the TADF properties of the polymers has been evaluated. The triplet energy and the delayed fluorescence contribution increases with increasing styrene content of the copolymers; meanwhile, the energy splitting between the singlet and triplet states (ΔE_{ST}) decreases with reducing styrene content of copolymers. OLED devices based these polymers as spin-coated emitting layers gave high performance, which is enhanced for the copolymers compared to the homopolymer. The best EL performance was achieved for the **Copo1**-based device with CE_{max} of 61.3 cd/A, PE_{max} of 40.1 lm/W, and EQE_{max} of 20.1%. To our knowledge this is the highest EQE reported to date for a TADF polymer.[26-31] Furthermore, at 100 cd m^{-2} the EQE was 5.3%. High EQE, even at very low luminance, is widely recognized as an important figure-of-merit for OLED efficiencies.[40] The key molecular features we have developed in this work, namely a non-conductive polymer backbone with pendant TADF units separated by non-emissive units, should be versatile for the design of new families of TADF polymers. It remains to be seen if polymers, which have

the potential benefits of high thermal stability, good film-forming ability and reduced phase separation, can be widely exploited for color tuning and enhanced TADF-OLED performance.

3. EXPERIMENTAL SECTION

Synthesis

Homopo. A mixture of 2-(10*H*-phenothiazin-10-yl)-8-vinyldibenzothiophene-*S*,*S*-dioxide[31] (600 mg, 1.37 mmol), AIBN (4 mg, 0.024 mmol), and toluene (15 mL) was placed in an ampule, which was cooled, degassed, and sealed *in vacuo*. After stirring at 60 ^{o}C for 48 h, the reaction mixture was poured into a large excess amount of methanol. The product which was obtained by filtration was dried *in vacuo*. The white polymer was fractionated by Soxhlet extraction using hexane. Yield: 550 mg (92%). ^{1}H-NMR ($CDCl_3$, 400 MHz) δ 0.5-2.6 (br, 3H), 6.0-8.2 (br, 12H, aromatic). Anal. Calcd. for $[C_{26}H_{17}NO_2S_2]_n$: C 71.07; H 3.87; N 3.19. Found: C 71.11; H 3.79, N 3.11%.

Copo 1-3. General procedure: a mixture of 2-(10*H*-phenothiazin-10-yl)-8-vinyldibenzothiophene-*S*,*S*-dioxide and styrene with different molar ratios, AIBN (10% mmol), and toluene (8.0 mL) / THF (20 mL) were placed in an ampule, which was cooled, degassed, and sealed *in vacuo*. After stirring at 60 ^{o}C for 20 h, the reaction mixture was poured into a large excess amount of methanol. The product which was obtained by filtration was dried *in vacuo*. The white polymer was fractionated by Soxhlet extraction using hexane.

Copo1: feed ratio (styrene and 2-(10*H*-phenothiazin-10-yl)-8-vinyldibenzothiophene-*S*,*S*-dioxide): 80:20. Yield: 85%. ^{1}HNMR ($CDCl_3$, 400 MHz) δ 7.9-6.1 (br, aromatic 84H), 2.0-0.8 (br, 30H). Anal. Calcd. for $\{[C_8H_8]_{63}\ [C_{26}H_{17}NO_2S_2]_{37}\}_n$: C 77.17; H 6.43; N 2.27. Found: C 77.28; H 6.36, N 2.26%.

Copo2: feed ratio (styrene and 2-(10*H*-phenothiazin-10-yl)-8-vinyldibenzothiophene-*S*,*S*-dioxide): 70:30. Yield: 88%. ^{1}HNMR ($CDCl_3$, 400 MHz) δ 7.9-6.0 (br, aromatic 92H), 2.0-0.8

(br, 30H). Anal. Calcd. for $\{[C_8H_8]_{54}\ [C_{26}H_{17}NO_2S_2]_{46}\}_n$: C 75.55; H 4.70; N 2.49. Found: C 75.66; H 4.59, N 2.51%.

Copo3: feed ratio (styrene and 2-(10*H*-phenothiazin-10-yl)-8-vinyldibenzothiophene-*S*,*S*-dioxide): 50:50. Yield: 86%. ^{1}HNMR ($CDCl_3$, 400 MHz) δ 7.9-5.9 (br, aromatic 112H), 2.0-0.8 (br, 30H). Anal. Calcd. for $\{[C_8H_8]_{33}\ [C_{26}H_{17}NO_2S_2]_{67}\}_n$: C 73.29; H 4.27; N 2.86. Found: C 73.37; H 4.19, N 2.84%.

Characterization

^{1}H NMR and ^{13}C NMR spectra were measured on a Bruker AV400 (400 MHz) spectrometer. Chemical shifts (δ) are given in parts per million (ppm) relative to tetramethylsilane (TMS; δ=0) as the internal reference. ^{1}H NMR spectra data are reported as chemical shift, relative integral, multiplicity (s = singlet, d = doublet, m = multiplet), coupling constant (*J* in Hz) and assignment. UV-Vis absorption spectra were recorded on a Hitachi U-2900 spectrophotometer. Differential scanning calorimetry (DSC) was performed on a TA Q2000 Differential Scanning Calorimeter at a heating rate of 10 ^{o}C min^{-1} from 25 to 300 ^{o}C under nitrogen atmosphere. The glass transition temperature (T_g) was determined from the second heating scan. Thermogravimetric analysis (TGA) was performed with a METTLER TOLEDO TGA/DSC 1/1100SF instrument. The thermal stability of the samples under a nitrogen atmosphere was determined by measuring their weight loss while heating at a rate of 10 ^{o}C min^{-1} from 25 to 800 ^{o}C. Cyclic voltammetry (CV) was carried out in nitrogen-purged acetonitrile at room temperature with a CHI 660E voltammetric analyzer. Tetrabutylammonium hexafluorophosphate ($TBAPF_6$) (0.1 M) was used as the supporting electrolyte. The conventional three-electrode configuration consisted of a glassy carbon working electrode, a platinum wire auxiliary electrode, and an Ag/AgCl pseudo-reference electrode with ferrocenium-ferrocene (Fc^+/Fc) as the internal standard. Cyclic voltammograms were obtained at scan rate of 50 mV s^{-1}. The onset potential was determined from the intersection of two tangents drawn at the rising and background currents of the cyclic voltammogram. Gel

permeation chromatography (GPC) analysis was carried out on a Waters 515-2410 system using polystyrene standards as molecular weight references and tetrahydrofuran (THF) as the eluent. Phosphorescence, prompt fluorescence (PF), and delayed emission (DF) spectra and decays were recorded using nanosecond gated luminescence and lifetime measurements (from 400 ps to 1 s) with either a high energy pulsed Nd:YAG laser emitting at 355 nm (EKSPLA) or a N2 laser emitting at 337 nm. Emission was focused onto a spectrograph and detected on a sensitive gated iCCD camera (Stanford Computer Optics) having sub-nanosecond resolution. PF/DF time resolved measurements were performed by exponentially increasing the gate and delay times.

Device fabrication and characterization. The hole-injection material PEDOT:PSS (8000), electron-transporting and hole-blocking material TPBI were obtained from commercial sources. ITO-coated glass with a sheet resistance of 10 Ω per square was used as the substrate. Before device fabrication, the ITO-coated glass substrate was precleaned and exposed to UV-ozone for 2 min. PEDOT:PSS was then spin-coated onto the clean ITO substrate as a hole-injection layer. Next a mixture of 10% polymer and 90% mCP in chlorobenzene was spin-coated (1 mg/mL;1500 rpm) to form a 45 nm thick emissive layer and annealed at 80 ^{o}C for 30 min to remove the residual solvent. Finally, a 30 nm thick electron-transporting layer of TPBi was vacuum deposited and a cathode composed of a 1 nm thick layer of LiF and aluminum (100 nm) was sequentially deposited onto the substrate through shadow masking with a pressure of 10^{-6} Torr. The current density-voltage-luminance (*J-V-L*) characteristics of the devices were measured using a Keithley 2400 Source meter and a Keithley 2000 Source multimeter. The EL spectra were recorded using a JYSPEX CCD3000 spectrometer. The EQE values were calculated from the luminance, current density, and electroluminescence spectrum according to previously reported methods. All measurements were performed at room temperature under ambient conditions.

SUPPORTING INFORMATION

^{1}H NMR spectra of the polymers; additional photophysical data. This information is available free of charge via the Internet at http://pubs.acs.org.

Acknowledgements. The financial support of the National Natural Science Foundations of China under Grant No. 51221002 is gratefully acknowledged. R.S.N. thanks the financial support from CAPES Foundation, Ministry of Education-Brazil, Grant BEX9474-13-7. M.R.B., F.B.D. and A.P.M. thank EPSRC (U.K.) grant EP/L02621X/1 for funding.

References

1. Pope, M.; Kallmann, H.; Magnante, P. Electroluminescence in Organic Crystals. *J. Chem. Phys.* **1963,** *38*, 2042-2043.
2. Helfrich, W.; Schneider, W. Recombination Radiation in Anthracene Crystals. *Phys. Rev. Lett.* **1965,** *14*, 229.
3. Tang, C. W.; VanSlyke, S. A. Organic Electroluminescent Diodes. *Appl. Phys. Lett.* **1987,** *51*, 913-915.
4. Chen, C. H.; Hsu, L. C.; Rajamalli, P.; Chang, Y. W.; Wu, F. I.; Liao, C. Y.; Chiu, M. J.; Chou, P. Y.; Huang, M. J.; Chu, L. K. Highly Efficient Orange and Deep-Red Organic Light Emitting Diodes with Long Operational Lifetimes Using Carbazole-Quinoline Based Bipolar Host Materials. *J. Mater. Chem. C.* **2014,** *2*, 6183-6191.
5. Su, T. H.; Fan, C. H.; Ou-Yang, Y. H.; Hsu, L. C.; Cheng, C. H. Highly Efficient Deep-Red Organic Electrophosphorescent Devices with Excellent Operational Stability Using Bis(indoloquinoxalinyl) Derivatives as the Host Materials. *J. Mater. Chem. C.* **2013,** *1*, 5084-5092.
6. Li, G.; Zhu, D.; Peng, T.; Liu, Y.; Wang, Y.; Bryce, M. R. Very High Efficiency Orange-Red Light-Emitting Devices with Low Roll-Off at High Luminance Based on an Ideal Host-Guest System Consisting of Two Novel Phosphorescent Iridium Complexes with Bipolar Transport. *Adv. Funct. Mater.* **2014,** *24*, 7420-7426.
7. Fukagawa, H.; Shimizu, T.; Hanashima, H.; Osada, Y.; Suzuki, M.; Fujikake, H. Highly Efficient and Stable Red Phosphorescent Organic Light-Emitting Diodes Using Platinum Complexes. *Adv. Mater.* **2012,** *24*, 5099-5103.

8. Friend, R.; Gymer, R.; Holmes, A.; Burroughes, J.; Marks, R.; Taliani, C.; Bradley, D.; Dos Santos, D.; Brédas, J.; Lögdlund, M. Conjugated Polymer Electroluminescence. *Nature* **1999,** *397*, 121-128.
9. Ma, Y.; Zhang, H.; Shen, J.; Che, C. Electroluminescence from Triplet Metal-Ligand Charge-Transfer Excited State of Transition Metal Complexes. *Synth. Met.* **1998,** *94*, 245-248.
10. Ikai, M.; Tokito, S.; Sakamoto, Y.; Suzuki, T.; Taga, Y. Highly Efficient Phosphorescence from Organic Light-Emitting Devices with an Exciton-Block Layer. *Appl. Phys. Lett.* **2001,** *79*, 156.
11. Tsuboyama, A.; Iwawaki, H.; Furugori, M.; Mukaide, T.; Kamatani, J.; Igawa, S.; Moriyama, T.; Miura, S.; Takiguchi, T.; Okada, S. Homoleptic Cyclometalated Iridium Complexes with Highly Efficient Red Phosphorescence and Application to Organic Light-Emitting Diode. *J. Am. Chem. Soc.* **2003,** *125*, 12971-12979.
12. Baldo, M. A.; O'Brien, D.; You, Y.; Shoustikov, A.; Sibley, S.; Thompson, M.; Forrest, S. Highly Efficient Phosphorescent Emission from Organic Electroluminescent Devices. *Nature* **1998,** *395*, 151-154.
13. Schmidbauer, S.; Hohenleutner, A.; König, B. Chemical Degradation in Organic Light-Emitting Devices: Mechanisms and Implications for the Design of New Materials. *Adv. Mater.* **2013,** *25*, 2114-2129.
14. Zhang, Q.; Li, J.; Shizu, K.; Huang, S.; Hirata, S.; Miyazaki, H.; Adachi, C. Design of Efficient Thermally Activated Delayed Fluorescence Materials for Pure Blue Organic Light Emitting Diodes. *J. Am. Chem. Soc.* **2012,** *134*, 14706-14709.
15. Rajamalli, P.; Senthilkumar, N.; Gandeepan, P.; Huang, P. Y.; Huang, M. J.; Ren-Wu, C. C.; Yang, C. Y.; Chiu, M. J.; Chu, L. K.; Lin, H. W. A New Molecular Design Based on Thermally Activated Delayed Fluorescence for Highly Efficient Organic Light Emitting Diodes. *J. Am. Chem. Soc.* **2016**. *138* (2), 628-634.
16. Dias, F. B.; Bourdakos, K. N.; Jankus, V.; Moss, K. C.; Kamtekar, K. T.; Bhalla, V.; Santos, J.; Bryce, M. R.; Monkman, A. P. Triplet Harvesting with 100% Efficiency By Way of Thermally Activated Delayed Fluorescence in Charge Transfer OLED Emitters. *Adv. Mater.* **2013,** *25*, 3707-3714.
17. Tao, Y.; Yuan, K.; Chen, T.; Xu, P.; Li, H.; Chen, R.; Zheng, C.; Zhang, L.; Huang, W. Thermally Activated Delayed Fluorescence Materials Towards the Breakthrough of Organoelectronics. *Adv. Mater.* **2014,** *26*, 7931-7958.
18. Adachi, C. Third-Generation Organic Electroluminescence Materials. *Jpn. J. Appl. Phys.* **2014,** *53*, 060101.

19. Zhang, Q.; Li, B.; Huang, S.; Nomura, H.; Tanaka, H.; Adachi, C. Efficient Blue Organic Light-Emitting Diodes Employing Thermally Activated Delayed Fluorescence. *Nat. Photonics* **2014,** *8*, 326-332.
20. Kim, B. S.; Lee, J. Y. Engineering of Mixed Host for High External Quantum Efficiency above 25% in Green Thermally Activated Delayed Fluorescence Device. *Adv. Funct. Mater.* **2014,** *24*, 3970-3977.
21. Arias, A. C.; MacKenzie, J. D.; McCulloch, I.; Rivnay, J.; Salleo, A. Materials and Applications for Large Area Electronics: Solution-Based Approaches. *Chem. Rev*. **2010,** *110*, 3-24.
22. Gong, S.; Yang, C.; Qin, J. Efficient Phosphorescent Polymer Light-Emitting Diodes by Suppressing Triplet Energy Back Transfer. *Chem. Soc. Rev.* **2012,** *41*, 4797-4807.
23. Cho, Y. J.; Yook, K. S.; Lee, J. Y. High Efficiency in a Solution-Processed Thermally Activated Delayed - Fluorescence Device Using a Delayed-Fluorescence Emitting Material with Improved Solubility. *Adv. Mater*. **2014,** *26*, 6642-6646.
24. Kim, Y. H.; Wolf, C.; Cho, H.; Jeong, S. H.; Lee, T. W. Highly Efficient, Simplified, Solution-Processed Thermally Activated Delayed-Fluorescence Organic Light-Emitting Diodes. *Adv. Mater*. **2016**, *28*, 734-741.
25. Rothe, C.; Monkman, A. Regarding the Origin of the Delayed Fluorescence of Conjugated Polymers. *J. Chem. Phys.* **2005,** *123*, 244904(1-6).
26. Albrecht, K.; Matsuoka, K.; Fujita, K.; Yamamoto, K. Carbazole Dendrimers as Solution-Processable Thermally Activated Delayed-Fluorescence Materials. *Angew. Chem., Int. Ed.* **2015,** *54*, 5677-5682.
27. Nikolaenko, A. E.; Cass, M.; Bourcet, F.; Mohamad, D.; Roberts, M. Thermally Activated Delayed Fluorescence in Polymers: A New Route Toward Highly Efficient Solution Processable OLEDs. *Adv. Mater.* **2015,** *27*, 7236-7240.
28. Luo, J.; Xie, G.; Gong, S.; Chen, T.; Yang, C. Creating a Thermally Activated Delayed Fluorescence Channel in a Single Polymer System to Enhance Exciton Utilization Efficiency for Bluish-Green Electroluminescence. *Chem. Commun.* **2016,** *52*, 2292-2295.
29. Lee, S. Y.; Yasuda, T.; Komiyama, H.; Lee, J.; Adachi, C. Thermally Activated Delayed Fluorescence Polymers for Efficient Solution-Processed Organic Light-Emitting Diodes. *Adv. Mater.* **2016**, *28*, 4019-4024.
30. Zhu, Y.; Zhang, Y.; Yao, B.; Wang, Y.; Zhang, Z.; Zhan, H.; Zhang, B.; Xie, Z.; Wang, Y.; Cheng, Y. Synthesis and Electroluminescence of a Conjugated Polymer with Thermally Activated Delayed Fluorescence. *Macromolecules* **2016**, *49*, 4373−4377.

31. Nobuyasu, R. S.; Ren, Z.; Griffiths, G. C.; Batsanov, A. S.; Data, P.; Yan, S.; Monkman, A. P.; Bryce, M. R.; Dias, F. B. Rational Design of TADF Polymers Using a Donor-Acceptor Monomer with Enhanced TADF Efficiency Induced by the Energy Alignment of Charge Transfer and Local Triplet Excited States. *Adv. Opt. Mater.* **2016**, *4*, 597-607.
32. Koene, B. E.; Loy, D. E.; Thompson, M. E. Asymmetric Triaryldiamines as Thermally Stable Hole Transporting Layers for Organic Light-Emitting Devices. *Chem. Mater.* **1998,** *10*, 2235-2250.
33. Cardona, C. M.; Li, W.; Kaifer, A. E.; Stockdale, D.; Bazan, G. C. Electrochemical Considerations for Determining Absolute Frontier Orbital Energy Levels of Conjugated Polymers for Solar Cell Applications. *Adv. Mater.* **2011,** *23*, 2367-2371.
34. Bredas, J. L. Mind the Gap! *Mater. Horiz.* **2014,** *1*, 17-19.
35. Dias, F. B. Kinetics of Thermal-Assisted Delayed Fluorescence in Blue Organic Emitters with Large Singlet-Triplet Energy Gap. *Phil. Trans. R. Soc. A* **2015,** *373*, 0447.
36. Gong, S.; He, X.; Chen, Y.; Jiang, Z.; Zhong, C.; Ma, D.; Jingui Qin, J.; Yang, C. Simple CBP Isomers with High Triplet Energies for Highly Efficient Blue Electrophosphorescence. *J. Mater. Chem*. **2012**, *22*, 2894-2899.
37. Lin, M.-S.; Yang, S.-J.; Chang, H.-W.; Huang, Y.-H.; Tsai, Y.-T.; Wu, C.-C.; Chou, S.-H.; Mondal, E.; Wong, K.-T. Incorporation of a CN Group into mCP: a New Bipolar Host Material for Highly Efficient Blue and White Electrophosphorescent Devices. *J. Mater. Chem.* **2012,** *22*, 16114-16120.
38. Tyson, D. S.; Castellano, F. N. Intramolecular Singlet and Triplet Energy Transfer in a Ruthenium (II) Diimine Complex Containing Multiple Pyrenyl Chromophores. *J. Phys. Chem. A.* **1999,** *103*, 10955-10960.
39. Zhang, Q.; Komino, T.; Huang, S.; Matsunami, S.; Goushi, K.; Adachi, C. Triplet Exciton Confinement in Green Organic Light-Emitting Diodes Containing Luminescent Charge-Transfer Cu(I) Complexes. *Adv. Funct. Mater.* **2012,** *22*, 2327-2336.
40. Jou, J-W.; Kumar, S.; Agrawal, A.; Li, T-H.; Sahoo, S. Approaches for Fabricating High Efficiency Organic Light Emitting Diodes. *J. Mater. Chem. C* **2015**, *3*, 2974-3002.